

Pressure versus concentration tuning of the superconductivity in $\text{Ba}(\text{Fe}_{1-x}\text{Co}_x)_2\text{As}_2$

Sandra Drotziger^{1,2}, Peter Schweiss¹, Kai Grube¹, Thomas Wolf¹, Peter Adelman¹,
Christoph Meingast¹, and Hilbert v. Löhneysen^{1,2}

¹ *Karlsruhe Institute of Technology, Institut für Festkörperphysik, PO Box 3640, D-76021 Karlsruhe, Germany*

² *Karlsruhe Institute of Technology, Physikalisches Institut, D-76128 Karlsruhe, Germany*

In the iron arsenide compound BaFe_2As_2 , superconductivity can be induced either by a variation of its chemical composition, e.g., by replacing Fe with Co, or by a reduction of the unit-cell volume through the application of hydrostatic pressure p . In contrast to chemical substitutions, pressure is expected to introduce no additional disorder into the lattice. We compare the two routes to superconductivity by measuring the p dependence of the superconducting transition temperature T_c of $\text{Ba}(\text{Fe}_{1-x}\text{Co}_x)_2\text{As}_2$ single crystals with different Co content x . We find that $T_c(p)$ of underdoped and overdoped samples increases and decreases, respectively, tracking quantitatively the $T_c(x)$ dependence. To clarify to which extent the superconductivity relies on distinct structural features we analyze the crystal structure as a function of x and compare the results with that of BaFe_2As_2 under pressure.

KEYWORDS: iron pnictide superconductors, Co-doped BaFe_2As_2 , superconductivity, high pressure

1. Introduction

In heavy-fermion compounds and cuprate perovskites unconventional superconductivity is observed close to magnetic order.¹⁾ The heavy-fermion compounds are intermetallics composed of $4f$ or $5f$ elements with superconducting transition temperatures of typically less than a few Kelvin. The cuprate high- T_c superconductors, on the other hand, are doped Mott-Hubbard insulators, composed of weakly coupled superconducting CuO_2 planes, and exhibit the highest T_c so far known, with values of more than 100 K. Recently, a family of new superconductors based on iron-pnictide layers has been discovered that might bridge the gap between these two material classes. In particular the 122 iron arsenides, $A\text{Fe}_2\text{As}_2$ ($A = \text{Ca}, \text{Sr}, \text{Ba}$), share the same tetragonal, ThCr_2Si_2 -type crystal structure (space group $I4/mmm$) with the prototypical heavy-fermion superconductor CeCu_2Si_2 while their relatively high T_c values, and the quasi-two-dimensional structure given by the weakly bonded, superconducting Fe_2As_2 layers are reminiscent of the cuprate perovskites. Superconductivity in 122 iron arsenides was first discovered in $\text{Ba}_{1-y}\text{K}_y\text{Fe}_2\text{As}_2$.²⁾ The parent compound BaFe_2As_2 exhibits collinear, anti-

ferromagnetic spin-density-wave order below $T_N \approx 140$ K together with a structural transition to an orthorhombic crystal structure (space group $Fmmm$).³⁾ When Ba is replaced with K these transitions split and are shifted to lower temperatures and superconductivity appears. With increasing K content, T_c grows and reaches its maximum of 38 K near the onset of magnetic order. In analogy to the heavy-fermion and cuprate superconductors, this has given rise to the conjecture that the superconducting pairing mechanism is essentially based on critical magnetic fluctuations. As a consequence, it was expected that any disorder should destroy the superconductivity, especially, if the superconducting gap has line or point nodes. An example for such a high sensitivity to impurities is the d -wave cuprate superconductor $\text{YBa}_2\text{Cu}_3\text{O}_{7-\delta}$.⁴⁾ Here, already 5% Zn in the superconducting CuO_2 planes suppress superconductivity completely. Unexpectedly, the substitution of Fe by Co in the 122 systems induces superconductivity with a qualitatively similar phase diagram as $\text{Ba}_{1-x}\text{K}_x\text{Fe}_2\text{As}_2$ but with a reduced T_c maximum of 24 K.^{5,6)} As the substitution of K or Co introduces holes or electrons into the system, respectively, it was suggested that the charge carrier concentration controls the superconductivity, similar to the cuprate superconductors. High-pressure experiments on the antiferromagnetic parent compounds $A\text{Fe}_2\text{As}_2$ ($A = \text{Ba}, \text{Sr}$) demonstrate, however, that—yet unidentified—structural changes alone are sufficient to induce superconductivity⁷⁻⁹⁾ resembling pressure induced superconductivity in heavy-fermion systems. Motivated by the fact that pressure does not introduce chemical disorder, in contrast to chemical substitutions, we investigated the pressure dependence of the superconductivity in $\text{Ba}(\text{Fe}_{1-x}\text{Co}_x)_2\text{As}_2$ to disentangle the effects of electron doping, structural changes, and disorder. As distinguished from most of the published high-pressure investigations we used magnetization instead of transport measurements to be able to identify the thermodynamic signature of superconductivity.

2. Sample Preparation and Experimental Methods

$\text{Ba}(\text{Fe}_{1-x}\text{Co}_x)_2\text{As}_2$ single crystals were grown with a Fe-As self-flux method in alumina crucibles.¹⁰⁾ The actual Co concentration x was determined by an XPS-microprobe analysis. To determine the crystal structure as a function of x we used X-ray diffraction analysis with a four-circle diffractometer and Mo K_α radiation at room temperature and $p = 0$. The subsequent structure refinement was performed with the aid of the SHELXS program. For the high-pressure magnetization measurements we built a miniaturized diamond-anvil cell that fits into a vibrating sample magnetometer (Oxford Instruments). The cell has an outer diameter of 12 mm and a length of 40 mm. To allow a maximum pressure of 10 GPa the diamond anvils have a culet diameter of less than 0.8 mm. The pressure cell is made from

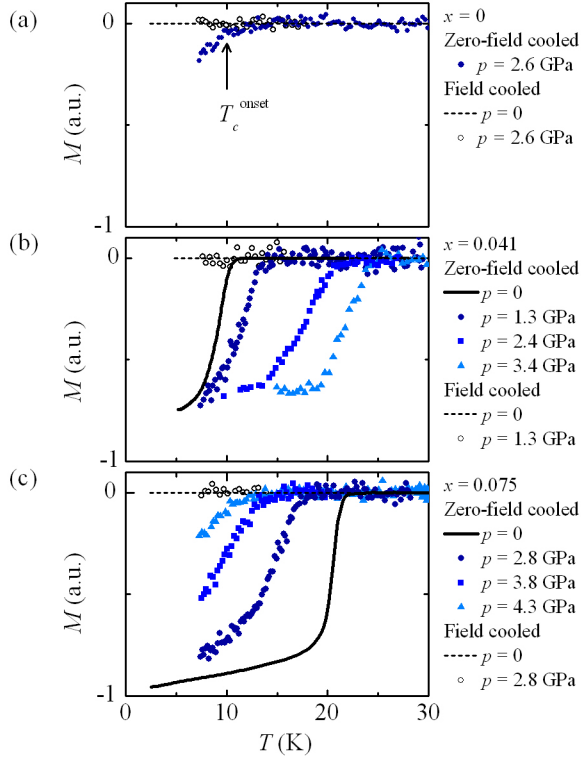


Fig. 1. (Color online) Zero-field-cooled and selected field-cooled magnetization measurements of $\text{Ba}(\text{Fe}_{1-x}\text{Co}_x)_2\text{As}_2$ single crystals with $x = 0$ (a), 0.041 (b), and 0.075 (c) in a magnetic field of $B = 5$ mT parallel to the c axis.

an annealed CuBe alloy to minimize any magnetic contributions. Due to the extremely small sample signal, however, the background signal of the paramagnetic cell material and the toolmarks from the manufacturing process cannot be neglected and have to be determined by separate measurements of the empty cell. To provide quasi-hydrostatic pressure conditions we used Daphne Oil 7373 (Idemitsu Co., Japan) as pressure-transmitting medium. Due to the difference between the thermal expansion of the cell body and the anvils the applied pressure varies by more than 10% between room temperature and 4 K. Therefore, we used a Raman spectrometer with a ^4He cooling stage to determine the pressure at $T_c(p)$ with the ruby-fluorescence method. The superconducting properties of the $\text{Ba}(\text{Fe}_{1-x}\text{Co}_x)_2\text{As}_2$ crystals were first studied at ambient pressure in a Quantum Design SQUID magnetometer. The diamagnetic shielding and Meissner effect was investigated with zero-field-cooled (ZFC) and field-cooled (FC) magnetization measurements with a magnetic field of 5 mT parallel to the c axis. Essentially, the Meissner signal (FC) was found to be negligible. From the crystals characterized in this way we cut small plate-like samples with typical dimensions of $50 \times 50 \times 20 \mu\text{m}^3$ and inserted them into the diamond-anvil cell. The subsequent experiments were

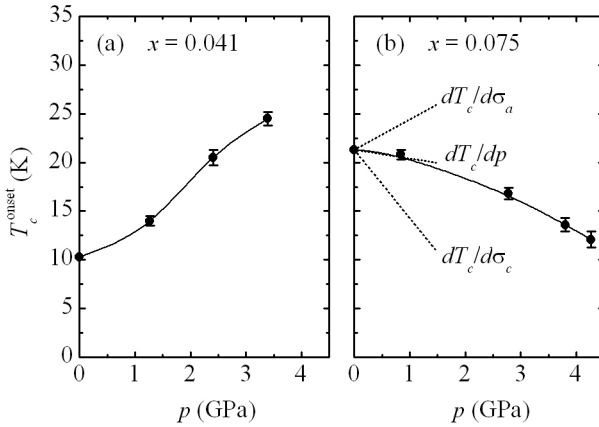


Fig. 2. The magnetic onset of the superconducting transition temperature versus pressure of $\text{Ba}(\text{Fe}_{1-x}\text{Co}_x)_2\text{As}_2$ single crystals with $x = 0.041$ (a) and 0.075 (b). The continuous lines are guides to the eyes. The dotted lines show the initial uniaxial and hydrostatic pressure dependences $dT_c/d\sigma_a = 3.1(1)$ K/GPa, $dT_c/d\sigma_c = -7.0(2)$ K/GPa, and $dT_c/dp = -0.9(3)$ K/GPa, respectively, obtained from specific heat and thermal expansion measurements.¹⁰⁾

carried out in the same manner as the ambient pressure measurements. The masses of the samples differ typically by 20%. Due to the difficulty to determine the exact mass of the samples used in the pressure cell it is impossible to give absolute magnetization values.

3. Magnetization Measurements

The magnetization data of the $\text{Ba}(\text{Fe}_{1-x}\text{Co}_x)_2\text{As}_2$ single crystals with $x = 0, 0.041$, and 0.075 are displayed in Fig. 1. As mentioned before, in our measurements the Meissner effect is significantly smaller than the diamagnetic shielding. This behavior seems to be characteristic for many iron arsenides and is usually attributed to strong flux trapping, possibly enforced by the random Co distribution.⁶⁾ As mentioned above, the parent compound BaFe_2As_2 has a normal-conducting, antiferromagnetic ground state. Figure 1(a) illustrates that a pressure of $2.6(1)$ GPa is sufficient to induce superconductivity with magnetically determined onset transition temperature of $T_c^{\text{onset}} \approx 10$ K. The sample with Co content of $x = 0.041$, shown in Fig. 1(b), is already superconducting at $p = 0$ with $T_c^{\text{onset}} \approx 11$ K. Under pressure its transition broadens and shifts to higher temperatures while the discontinuity ΔM at T_c remains roughly constant. The overdoped sample with $x = 0.075$ and a $T_c^{\text{onset}}(p = 0)$ of ≈ 21.5 K shows the opposite behavior: Here, T_c drops with increasing pressure (see Fig. 1(c)). The strong diamagnetic shielding of the $x = 0.041$ and 0.075 crystals and the consistence of their T_c^{onset} values with other thermodynamic measurements clearly indicate bulk superconductivity,^{10,11)} although—in particular at low Co concentrations—a normal-conducting volume fraction can-

not be ruled out. The broadening of the transitions at high pressures might be due to a small, slowly increasing uniaxial pressure contribution due to a gradual loss of the hydrostacity of the pressure-transmitting medium.

In Fig. 2 we summarize the measured T_c^{onset} values as a function of p . The initial pressure dependence of the $x = 0.041$ sample with $dT_c^{\text{onset}}/dp \approx 2.9(2)$ K/GPa is supported by recent resistivity measurements which have been performed in a smaller pressure range on samples with different Co concentrations.¹²⁾ At high doping levels, on the other hand, these measurements reveal nearly no change of T_c under pressure in contrast to our measurement of the $x = 0.075$ sample. With increasing Co content the T_c values determined by transport and thermodynamic measurements start to deviate from each other, indicating minority superconducting phases with higher T_c than the majority bulk phase of Co concentration x (see the difference between the open and closed symbols in Fig. 3(a)). These differences can be attributed to the sensitivity of resistivity measurements to filamentary superconductivity as opposed to bulk measurements of thermodynamic properties such as magnetization, thermal expansion, and specific heat. Indeed, the initial slope $dT_c^{\text{onset}}/dp = -0.7(2)$ K/GPa of the $x = 0.075$ sample, obtained from our magnetization data, is convincingly confirmed by thermal expansion and specific heat measurements on a sample of the same batch. The Ehrenfest relations allow the determination of the uniaxial and hydrostatic pressure dependences of T_c at $p = 0$ from these data (see the dotted lines in Fig. 2(b)).¹⁰⁾ In view of the strongly anisotropic uniaxial pressure dependences this excellent agreement proves that our data reflect indeed thermodynamic bulk properties, $dT_c^{\text{onset}}/dp = dT_c/dp$, under hydrostatic pressure conditions.

The $x = 0.041$ concentration is at the underdoped and the $x = 0.075$ at the overdoped side of the phase diagram where T_c grows and drops with x , respectively. Hence, the sign change of dT_c/dp mirrors that of dT_c/dx . To compare both effects quantitatively we assume that the T_c change with p is proportional to that with x (see Fig. 3(a)). Surprisingly, the data collapse on a single phase line if the proportionality constant is set to $\Delta p/\Delta x \approx 1.275$ GPa/at.%Co. This scaling property of pressure and doping in the Fe₂As₂ planes is in remarkable contrast to the behavior found for cuprate superconductors where minute amounts of Zn in the CuO₂ planes quickly suppress superconductivity. On the other hand, a similar scaling of $T_c(p)$ and $T_c(x)$ at smaller doping levels was observed for Cd-doped CeCoIn₅ where Cd occupies the In sites.²³⁾ Substitution of magnetic and nonmagnetic ions into the Ce sublattice, however, leads likewise to a rapid reduction of T_c .²⁴⁾ A strong suppression of T_c by nonmagnetic as well as magnetic impurities is a hallmark of unconventional, non-*s*-wave superconductivity.²⁵⁾ Usually, T_c approaches zero when the charge carrier mean free path becomes smaller than

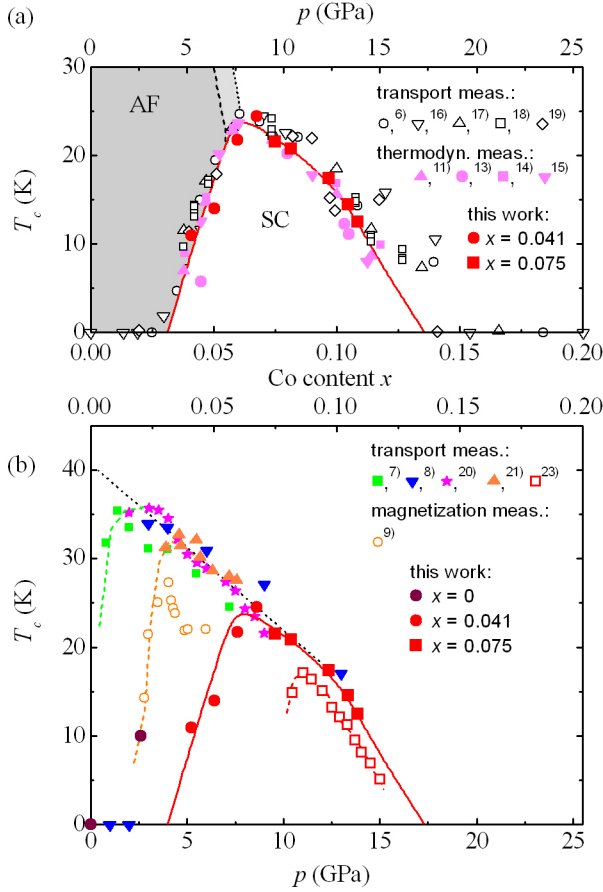


Fig. 3. (Color online) (a) Phase diagram of $\text{Ba}(\text{Fe}_{1-x}\text{Co}_x)_2\text{As}_2$ as a function of x (lower scale) at $p = 0$. The dotted and dashed lines denote the structural and magnetic transitions, respectively. At $x > 0.06$, there is an increasing deviation between T_c values determined by thermodynamic properties^{11,13–15}) and transport measurements.^{6,16–19}) The x values of the data from Ref.¹⁵) are scaled to match the T_c maximum. To compare the T_c dependence on x and p , we plot our $T_c(p)$ values of $x = 0.041$ and 0.075 in the same phase diagram as a function of p (upper scale) by assuming $\Delta p/\Delta x \approx 1.275$ GPa/at.%Co. The solid line is a guide to the eye. (b) Comparison of our measurements with high-pressure data of the undoped parent compound. These are resistivity^{7,8,20–22}) and magnetization measurements.⁹) The solid phase line $T_c(x, p = 0)$ is taken from (a). The dashed lines illustrate the different, pressure-induced superconductivity onsets. The dotted line is a linear extrapolation of the high-pressure data to $p = 0$.

the superconducting coherence length ξ . Recent μSR measurements demonstrate that at low Co content superconductivity develops in small islands around the randomly distributed Co ions.²⁶) For optimally doped $\text{Ba}(\text{Fe}_{1-x}\text{Co}_x)_2\text{As}_2$, ξ is of the order of the a axis lattice parameter and, hence, larger than the mean Fe-Fe nearest-neighbor distance $\approx a/\sqrt{2(1-x)}$ (see Fig. 4(a)).^{27,28}) The fact that samples with smaller Co concentration under pressure match those of larger x at $p = 0$, especially at the T_c maximum, proves that chemical disorder does

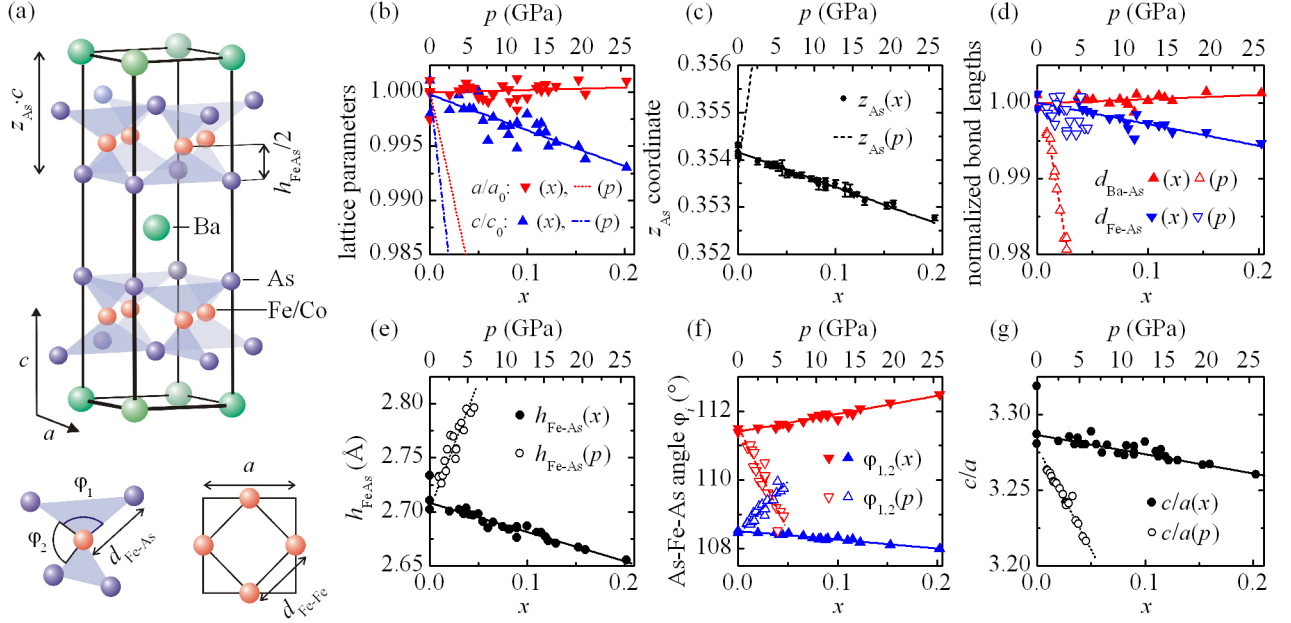


Fig. 4. (Color online) (a) The tetragonal crystal structure of $\text{Ba}(\text{Fe}_{1-x}\text{Co}_x)_2\text{As}_2$. (b) The a and c axis divided by $a_0 = 3.966 \text{ \AA}$ and $c_0 = 13.037 \text{ \AA}$, respectively, and the As z coordinate (c) as a function of x (lower scale) at $p = 0$. The broken lines represent the behavior of a , c , and z_{As} of BaFe_2As_2 under pressure from Ref.²⁹⁾ plotted as a function of p (upper scale) with the proportionality constant from Fig. 3. (d) The Ba-As and $(\text{Fe}_{1-x}\text{Co}_x)$ -As bond lengths divided by 3.374 \AA and 2.392 \AA , respectively, the Fe_2As_2 layer thickness $h_{\text{Fe-As}}$ (e), the As-Fe-As bond angles ϕ_i (f), and the c/a ratio (d). The open symbols represent the corresponding quantities of BaFe_2As_2 under pressure.²⁹⁾ All lines are linear fits to the data points.

not affect the transition temperature which is consistent with fully gapped superconductivity. It is instructive to compare the T_c values of Co doped samples with those of the undoped parent compound BaFe_2As_2 under pressure (see Fig. 3(b)). In comparison to the Co doped samples under pressure, the various published $T_c(p)$ data of pure BaFe_2As_2 differ strongly at low pressures. As pointed out by Duncan *et al.*,³⁰⁾ already tiny amounts of uniaxial pressure can suppress the magnetic order and shift the onset of superconductivity to lower pressures. Consequently, the degree of hydrostaticity of the pressure-transmitting medium used has a crucial effect on the measurement. It is reassuring that our $x = 0$ data coincides with those of Alireza *et al.*⁹⁾ who used the same pressure medium. (Since pressure inhomogeneities tend to increase with applied pressure, the higher reproducibility of the experiments on Co-doped samples are partly a result of the lower maximal pressures needed to observe significant T_c changes.) The extremely high sensitivity of the orthorhombic phase to stress, typical of heavily twinned crystals,^{31,32)} might be considerably reduced if the Co ions act as pinning centers

for the twin boundaries.^{33,34)} Indeed, all high-pressure experiments on BaFe_2As_2 that succeeded to suppress the twinned, orthorhombic phase show superconductivity with the same pressure dependence of T_c . In accordance with the observed scaling between x and p , they all merge into the phase boundary $T_c(x \cdot \Delta p / \Delta x)$ of the doped samples at $p = 0$. A similar decoupling of the magnetostructural and superconducting transitions together with a common phase boundary at high doping levels has been reported for $\text{Ba}(\text{Fe}_{1-x}\text{M}_x)_2\text{As}_2$ with $\text{M} = \text{Co}, \text{Ni}, \text{Rh},$ and Pd , if T_c is plotted against the doped extra electron at the Fe/M site or the c/a ratio.¹⁷⁾ Notably, in both examples the measurements tend to delineate a uniform phase line, irrespective of the different endpoints of magnetic order, as illustrated in Fig. 3(b). Since the difference of endpoints does not result in a corresponding shift of the entire superconducting “dome”, the superconductivity cannot originate from the magnetostructural instability but is rather expelled by the onset of antiferromagnetic order due to the strong competition of the different ground states. If the T_c dependence of the overdoped and optimally doped regime is extrapolated to p (or x) = 0, the maximal T_c would amount to 40 K, a value which is close to the highest T_c found in doped 122 iron arsenides.²⁾

4. Search for Structural key parameters

The fact that superconductivity can be induced by hydrostatic pressure without doping suggests that distinct structural parameters control the ground state, in loose analogy to the f -atom separation in some heavy-fermion superconductors. The currently most promising key parameters are the c/a ratio,^{10,17)} the next nearest Fe-Fe distance $d_{\text{Fe-Fe}} = a/\sqrt{2}$,^{35,36)} the Fe_2As_2 layer thickness h_{FeAs} (or pnictogen “height” $h_{\text{FeAs}}/2$),³⁷⁻⁴⁰⁾ and the As-Fe-As bond angles ϕ_i ($i = 1,2$) of the tetragonal structure.^{35,41)} Theoretical studies pointed out that magnetically mediated superconductivity favors quasi-two-dimensional structures.¹⁾ Indeed, most of the discovered unconventional superconductors are characterized by strong magnetic and electronic anisotropies and comprise layered, superconducting building blocks. The heavy-fermion superconductors based on the HoCoGa_5 structure show even a linear relationship between T_c and the ratio of the tetragonal lattice parameters c/a .⁴²⁾ As already shown in Ref.,¹⁰⁾ the uniaxial pressure dependences of T_c , depicted in Fig. 2, support a similarly strong influence of the c/a ratio on superconductivity in the 122 iron-arsenide superconductors. The As-Fe-As bond angles (and h_{FeAs}), on the other hand, are suggested to control the density of states at the Fermi level, with the highest T_c observed for an ideal tetrahedral angle of 109.47° , where ϕ_1 and ϕ_2 become equal. An example for the important effect of ϕ_i might be given by the hole-doped $\text{Ba}_{1-y}\text{K}_y\text{Fe}_2\text{As}_2$. This compound exhibits in addition a similar change

of ϕ_i and $d_{\text{Fe-Fe}}$ under pressure and doping with K.²⁹⁾ Together with its related compound $\text{Sr}_{1-y}\text{K}_y\text{Fe}_2\text{As}_2$, it shows an approximate correlation between dT_c/dy and dT_c/dp .^{43,44)}

Based on the equivalence between $T_c(p)$ and $T_c(x \cdot \Delta p / \Delta x)$ found in $\text{Ba}(\text{Fe}_{1-x}\text{Co}_x)_2\text{As}_2$, we are now able to check the relevance of the suggested structural parameters for the electron-doped 122 compounds. For this we analyzed the crystal structure of $\text{Ba}(\text{Fe}_{1-x}\text{Co}_x)_2\text{As}_2$ as a function of x at room temperature and $p = 0$ and compare it with BaFe_2As_2 measured under pressure at $T = 150 \text{ K}$.²⁹⁾ The temperature difference between the data sets can be neglected because the thermal expansion is small compared to the pressure and doping dependent changes.²⁹⁾ The structure is fully characterized by the lattice parameters a , c , and the z coordinate of the As ion. In Fig. 4(b) and (c) these parameters are plotted against x and p using the proportionality constant from above. In accordance to other Co-doped iron arsenides,⁴⁵⁾ both axes exhibit only small, gradual changes, demonstrating homogeneous solid $\text{Ba}(\text{Fe}_{1-x}\text{Co}_x)_2\text{As}_2$ solutions up to $x = 0.2$. With increasing x , the a axis remains nearly unchanged and the c axis exhibits a slight shrinkage, which is exclusively caused by a decrease of h_{FeAs} , as indicated by the drop of $z_{\text{As}}(x)$ in Fig. 4(c). In contrast, pressure leads to a shortening of both axes and an increase of $z_{\text{As}}(p)$.^{29,46)} The dissimilar behavior of z_{As} as a function of p and x originates from the different compressibilities of the Ba-As and $(\text{Fe}_{1-x}\text{Co}_x)$ -As bonds. As shown by Fig. 4(d), Co substitution leads to a tiny decrease of the $(\text{Fe}_{1-x}\text{Co}_x)$ -As bond $d_{\text{Fe-As}}$ while the Ba-As distance $d_{\text{Ba-As}}$ increases slightly. Under pressure, too, the Fe-As bond hardly changes but the weak Ba-As bond exhibits a pronounced reduction. The staggered structure of the incompressible Fe-As bonds forms “Nuremberg scissors” so that under hydrostatic pressure the compression of the Fe_2As_2 layer along the a axis leads to an increase of the layer thickness parallel to c , as shown in Fig. 4(e). This has the additional effect that with growing x the As-Fe-As angles reveal an increasing deviation from the ideal tetrahedral angle (see Fig. 4(f)). In contrast to the application of pressure or doping with K, $\text{Ba}(\text{Fe}_{1-x}\text{Co}_x)_2\text{As}_2$ exhibits its T_c maximum for a structure that is far away from that of a regular Fe-As tetrahedron. Finally we turn to the c/a ratio displayed in Fig. 4(g). Although both, x and p lead to a decrease of c/a , the slopes differ by nearly one order of magnitude. It has, however, taken into account that a change of c/a might affect—apart from the effective dimensionality—the charge carrier density due to a simultaneous change of the bond angles ϕ_i , as already suggested in Ref.¹⁰⁾ To disentangle both effects we compare the T_c values of different Co-doped 122 compounds $A(\text{Fe}_{1-x}\text{Co}_x)_2\text{As}_2$ with $A = \text{Ca}$,⁴⁷⁾ Sr ,⁴⁸⁾ Eu ,⁴⁹⁾ and Ba . The different A ion radii result in a variation of their c/a ratio that ranges from 3.01 to 3.28 for $A = \text{Ca}$ and Ba , respectively. All mentioned Co-doped compounds show the T_c maximum

approximately at the same Co concentration and, consequently, at the same charge carrier concentration. Therefore, the T_c maximum as a function of c/a should reflect the dependence on the effective dimensionality. Compared to the application of pressure and doping with Co, which show a T_c dependence of $dT_c(p)/d(c/a) \approx 200$ K and $dT_c(x)/d(c/a) \approx 1400$ K, respectively, the in this way determined variation of T_c at a fixed charge-carrier concentration is insignificantly small $dT_c(A)/d(c/a) \approx 13$ K. This observation corresponds to the aforementioned electron-doped $\text{Ba}(\text{Fe}_{1-x}\text{M}_x)_2\text{As}_2$ ($M = \text{Co}, \text{Rh}, \text{Ni}, \text{Pt}$). It demonstrates that c/a is predominately determined by the additional electrons doped at the Fe/ M site. Obviously, in contrast to our expectation, the interlayer distance and hence the dimensionality have nearly no effect on superconductivity.

As a result neither the Fe-Fe distance $d_{\text{Fe-Fe}}$, nor the bond angles ϕ_i , nor the Fe_2As_2 layer thickness (pnictogen height) $h_{\text{Fe-As}}$, nor the c/a ratio meet the criteria for structural key parameters. The only parameter which might show a similar behavior with x and p is the Fe/Co-As bond length $d_{\text{Fe-As}}$, although additional experimental studies are necessary to prove whether the $d_{\text{Fe-As}}$ exhibits a comparable slight reduction under high pressure as with large Co concentrations. Recently, the importance of $d_{\text{Fe-As}}$ was pointed out by crystal structure investigations of electron and hole-doped 122 compounds which indicate that superconductivity favors a distinct Fe/ M -As bond length.⁵⁰⁾ First principle calculations show that $d_{\text{Fe-As}}$ determines the local magnetic moment on the Fe site.⁵¹⁾ Due to its magnetostrictive nature a vanishing moment would be reflected in a pronounced reduction of $d_{\text{Fe-As}}$. In contrast to the experimentally determined values, the first-principle calculations predict for the optimized structure, without accounting for magnetism, a clearly smaller Fe/Co-As bond length. The fact that $d_{\text{Fe-As}}$ is large was taken as a hint for large magnetic moments and frustrated magnetic interactions.^{52,53)} As in addition $d_{\text{Fe-As}}$ exhibits only minor changes with increasing x and p , even if the system reveals no longer magnetic order, the superconductivity has to evolve from a paramagnetic phase with strong magnetic fluctuations. In all iron-arsenides discovered so far the temperature of the magnetic transition is equal or smaller than that of the structural transformation. Apparently, the orthorhombic distortion is a prerequisite for long-range magnetic order, possibly due to the frustration of two antiferromagnetic sublattices.⁵⁴⁾ Taking this into account the phase diagrams depicted in Figure 3(b) show that as soon as the structural transition is suppressed by pressure superconductivity replaces antiferromagnetism. Therefore, both, magnetic order and superconductivity seem to originate from the same, presumably magnetic interactions.

5. Summary

In conclusion we found a scaling of the phase diagram of $\text{Ba}(\text{Fe}_{1-x}\text{Co}_x)_2\text{As}_2$ with electron doping by Co or pressure. This gives rise to the assumption that distinct structural parameters are essential in achieving superconductivity. A detailed comparison of the key elements suggested so far reveals, however, a different, often even opposite, evolution of these parameters under pressure and Co-doping. The only exception might be given by the Fe-As bond length. Its insensitivity to p and x , however, requires additional high-resolution crystal-structure investigations to demonstrate a clear correlation to superconductivity. The discovered similarities should be useful to discriminate between different theoretical models. In this context, the study of 122 iron arsenides with other chemical substitutions under pressure and additional studies of the anisotropic uniaxial pressure dependence of T_c would be helpful. The insensitivity of superconductivity to any chemical disorder clearly points to a nodeless superconducting gap. The decoupling of the magnetostructural and superconducting transitions and the uniform phase boundary at high pressure or high doping levels indicate a strong competition of the ground states and disfavor the antiferromagnetic quantum phase transition as source for superconductivity. The rigid Fe-As bond, on the other hand, makes clear that even outside the antiferromagnetic phase magnetic interactions are present and that magnetic order and superconductivity might have a common origin in the 122 iron arsenides.

Acknowledgments

We acknowledge financial support through the Helmholtz association (VIRQ VH-VI-127) and the Deutsche Forschungsgemeinschaft (SPP 1458).

References

- 1) P. Monthoux, D. Pines, and G. G. Lonzarich: *Nature* **450** (2007) 1177.
- 2) M. Rotter, M. Pangerl, M. Tegel, and D. Johrendt: *Angew. Chem. Int. Ed.* **47** (2008) 7949.
- 3) Q. Huang, Y. Qiu, W. Bao, M. A. Green, J. W. Lynn, Y. C. Gasparovic, T. Wu, G. Wu, and X. H. Chen: *Phys. Rev. Lett.* **101** (2008) 257003.
- 4) B. Jayaram, S. K. Agarwal, C. V. Narasimha Rao, and A. V. Narlikar: *Phys. Rev. B* **38** (1988) 2903.
- 5) A. S. Sefat, R. Jin, M. A. McGuire, B. C. Sales, D. J. Singh, and D. Mandrus: *Phys. Rev. Lett.* **101** (2008) 117004.
- 6) J.-H. Chu, J. G. Analytis, C. Kucharczyk, and I. R. Fisher: *Phys. Rev. B* **79** (2009) 014506.
- 7) A. Mani, N. Ghosh, S. Paulraj, A. Bharathi, and C. S. Sundar: *Europhys. Lett.* **87** (2009) 17004.
- 8) H. Fukazawa, N. Takeshita, T. Yamazaki, K. Kondo, K. Hirayama, Y. Kohori, K. Miyazawa, H. Kito, H. Eisaki, and A. Iyo: *J. Phys. Soc. Jpn.* **77** (2008) 105004.
- 9) P. L. Alireza, Y. T. C. Ko, J. Gillett, C. M. Petrone, J. M. Cole, G. G. Lonzarich, and S. E. Sebastian: *J. Phys.: Condens. Matter* **21** (2009) 012208.
- 10) F. Hardy, P. Adelman, T. Wolf, H. v. Löhneysen, and C. Meingast: *Phys. Rev. Lett.* **102** (2009) 187004.
- 11) S. L. Bud'ko, N. Ni, and P. C. Canfield: *Phys. Rev. B* **79** (2009) 220516.
- 12) K. Ahilan, F. L. Ning, T. Imai, A. S. Sefat, M. A. McGuire, B. C. Sales, and D. Mandrus: *Phys. Rev. B* **79** (2009) 214520.
- 13) K. Gofryk, A. S. Sefat, M. A. McGuire, B. C. Sales, D. Mandrus, J. D. Thompson, E. D. Bauer, and F. Ronning: *Phys. Rev. B* **81** (2010) 184518.
- 14) R. Prozorov, M. Tanatar, E. Blomberg, P. Prommapan, R. Gordon, N. Ni, S. Bud'ko, and P. Canfield: *Physica C* **469** (2009) 667.
- 15) M. Gang, Z. Bin, C. Peng, W. Zhao-Sheng, F. Lei, S. Bing, S. Lei, R. Cong, and W. Hai-Hu: *Chinese Physics Letters* **27** (2010) 037402.
- 16) F. Rullier-Albenque, D. Colson, A. Forget, and H. Alloul: *Phys. Rev. Lett.* **103** (2009) 057001.
- 17) P. C. Canfield, S. L. Bud'ko, N. Ni, J. Q. Yan, and A. Kracher: *Phys. Rev. B* **80** (2009) 060501.
- 18) J.-P. Reid, M. A. Tanatar, X. G. Luo, H. Shakeripour, N. Doiron-Leyraud, N. Ni, S. L. Bud'ko, P. C. Canfield, R. Prozorov, and L. Taillefer: *Phys. Rev. B* **82** (2010) 064501.
- 19) F. L. Ning, K. Ahilan, T. Imai, A. S. Sefat, M. A. McGuire, B. C. Sales, D. Mandrus, P. Cheng, B. Shen, and H.-H. Wen: *Phys. Rev. Lett.* **104** (2010) 037001.
- 20) F. Ishikawa, N. Eguchi, M. Kodama, K. Fujimaki, M. Einaga, A. Ohmura, A. Nakayama, A. Mitsuda, and Y. Yamada: *Phys. Rev. B* **79** (2009) 172506.
- 21) E. Colombier, S. L. Bud'ko, N. Ni, and P. C. Canfield: *Phys. Rev. B* **79** (2009) 224518.
- 22) T. Yamazaki, N. Takeshita, R. Kobayashi, H. Fukazawa, Y. Kohori, K. Kihou, C.-H. Lee, H. Kito, A. Iyo, and H. Eisaki: *Phys. Rev. B* **81** (2010) 224511.
- 23) L. D. Pham, T. Park, S. Maquilon, J. D. Thompson, and Z. Fisk: *Phys. Rev. Lett.* **97** (2006) 056404.
- 24) J. Paglione, T. A. Sayles, P.-C. Ho, J. R. Jeffries, and M. B. Maple: *Nature Phys.* **3** (2007) 703.
- 25) A. P. Mackenzie, R. K. W. Haselwimmer, A. W. Tyler, G. G. Lonzarich, Y. Mori, S. Nishizaki, and Y. Maeno: *Phys. Rev. Lett.* **80** (1998) 161.

- 26) S. Takeshita, R. Kadono, M. Hiraishi, M. Miyazaki, A. Koda, S. Matsuishi, and H. Hosono: *Phys. Rev. Lett.* **103** (2009) 027002.
- 27) A. Yamamoto, J. Jaroszynski, C. Tarantini, L. Balicas, J. Jiang, A. Gurevich, D. C. Larbalestier, R. Jin, A. S. Sefat, M. A. McGuire, B. C. Sales, D. K. Christen, and D. Mandrus: *Appl. Phys. Lett.* **94** (2009) 062511.
- 28) Y. Yin, M. Zech, T. L. Williams, X. F. Wang, G. Wu, X. H. Chen, and J. E. Hoffman: *Phys. Rev. Lett.* **102** (2009) 097002.
- 29) S. A. J. Kimber, A. Kreyssig, Y.-Z. Zhang, H. O. Jeschke, R. Valenti, F. Yokaichiya, E. Colombier, J. Yan, T. C. Hansen, T. Chatterji, R. J. McQueeney, P. C. Canfield, A. I. Goldman, and D. N. Argyriou: *Nat. Mater.* **8** (2009) 471.
- 30) W. J. Duncan, O. P. Welzel, C. Harrison, X. F. Wang, X. H. Chen, F. M. Grosche, and P. G. Niklowitz: *J. Phys.: Condens. Matter* **22** (2010) 052201.
- 31) K. Grube, W. H. Fietz, U. Tutsch, O. Stockert, and H. v. Löhneysen: *Phys. Rev. B* **60** (1999) 11947.
- 32) S. L. Bud'ko, N. Ni, S. Nandi, G. M. Schmiedeshoff, and P. C. Canfield: *Phys. Rev. B* **79** (2009) 054525.
- 33) M. A. Tanatar, A. Kreyssig, S. Nandi, N. Ni, S. L. Bud'ko, P. C. Canfield, A. I. Goldman, and R. Prozorov: *Phys. Rev. B* **79** (2009) 180508.
- 34) T.-M. Chuang, M. P. Allan, J. Lee, Y. Xie, N. Ni, S. L. Bud'ko, G. S. Boebinger, P. C. Canfield, and J. C. Davis: *Science* **327** (2010) 181.
- 35) J. Zhao, Q. Huang, C. de la Cruz, S. Li, J. W. Lynn, Y. Chen, M. A. Green, G. F. Chen, G. Li, Z. Li, J. L. Luo, N. L. Wang, and P. Dai: *Nat. Mater.* **7** (2008) 953.
- 36) K. Miyazawa, K. Kihou, P. M. Shirage, C.-H. Lee, H. Kito, H. Eisaki, and A. Iyo: *J. Phys. Soc. Jpn.* **78** (2009) 034712.
- 37) D. J. Singh: *Phys. Rev. B* **78** (2008) 094511.
- 38) Y. Mizuguchi, Y. Hara, K. Deguchi, S. Tsuda, T. Yamaguchi, K. Takeda, H. Kotegawa, H. Tou, and Y. Takano: *Supercond. Sci. Technol.* **23** (2010) 054013.
- 39) K. Kuroki, H. Usui, S. Onari, R. Arita, and H. Aoki: *Phys. Rev. B* **79** (2009) 224511.
- 40) E. Kuchinskii, I. Nekrasov, and M. Sadoyskii: *JETP Letters* **91** (2010) 518.
- 41) C.-H. Lee, A. Iyo, H. Eisaki, H. Kito, M. T. Fernandez-Diaz, T. Ito, K. Kihou, H. Matsuhata, M. Braden, and K. Yamada: *J. Phys. Soc. Jpn.* **77** (2008) 083704.
- 42) E. D. Bauer, J. D. Thompson, J. L. Sarrao, L. A. Morales, F. Wastin, J. Rebizant, J. C. Griveau, P. Javorsky, P. Boulet, E. Colineau, G. H. Lander, and G. R. Stewart: *Phys. Rev. Lett.* **93** (2004) 147005.
- 43) M. S. Torikachvili, S. L. Bud'ko, N. Ni, and P. C. Canfield: *Phys. Rev. B* **78** (2008) 104527.
- 44) M. Gooch, B. Lv, B. Lorenz, A. M. Guloy, and C.-W. Chu: *Phys. Rev. B* **78** (2008) 180508.
- 45) A. Marcinkova, D. A. M. Grist, I. Margiolaki, T. C. Hansen, S. Margadonna, and J.-W. G. Bos: *Phys. Rev. B* **81** (2010) 064511.
- 46) J.-E. Jorgensen, J. S. Olsen, and L. Gerward: *Solid State Commun.* **149** (2009) 1161.
- 47) N. Kumar, R. Nagalakshmi, R. Kulkarni, P. L. Paulose, A. K. Nigam, S. K. Dhar, and A. Thamizhavel: *Phys. Rev. B* **79** (2009) 012504.
- 48) A. Leithe-Jasper, W. Schnelle, C. Geibel, and H. Rosner: *Phys. Rev. Lett.* **101** (2008) 207004.

- 49) J. J. Ying, T. Wu, Q. J. Zheng, Y. He, G. Wu, Q. J. Li, Y. J. Yan, Y. L. Xie, R. H. Liu, X. F. Wang, and X. H. Chen: Phys. Rev. B **81** (2010) 052503.
- 50) J. S. Kim, S. Khim, H. J. Kim, M. J. Eom, J. M. Law, R. K. Kremer, J. H. Shim, and K. H. Kim: Phys. Rev. B **82** (2010) 024510.
- 51) M. D. Johannes, I. I. Mazin, and D. S. Parker: Phys. Rev. B **82** (2010) 024527.
- 52) T. Yildirim: Physica C **469** (2009) 425.
- 53) I. I. Mazin and M. D. Johannes: Nature Phys. **5** (2009) 141.
- 54) T. Yildirim: Phys. Rev. Lett. **101** (2008) 057010.